The decarbonization of coal tar via microwave-initiated catalytic deep dehydrogenation

Yuqiang Yan [a, b], Sergio Gonzalez-Cortes [b], Benzhen Yao [b], Xiangyu Jie [b], Hamid AlMegren [c],

*Fahai Cao [a, *], Jon Dilworth [b], Daniel R. Slocombe [d], Tiancun Xiao [b, *], Peter P. Edwards [b, *]*

[a] School of Chemical Engineering, East China University of Science and Technology, Shanghai 200237, China

[b] King Abdulaziz City for Science and Technology-Oxford Centre of Excellence for Petrochemicals (KOPRC), Inorganic Chemistry Laboratory, Department of Chemistry, University of Oxford, Oxford OX1 3QR, UK

[c] Materials Division, King Abdulaziz City for Science and Technology, P.O. Box 6086, Riyadh 11442, Kingdom of Saudi Arabia

[d] School of Engineering, Cardiff University, Queen's Buildings, The Parade, Cardiff CF24 3AA, UK

*Corresponding author.

Email: Peter P. Edwards (peter.edwards@chem.ox.ac.uk) or to Tiancun Xiao (xiao.tiancun@chem.ox.ac.uk).

ABSTRACT

Coal tar, a major by-product of the coal industry, presents considerable difficulties in its refining and conversion into fuels due to its complex chemical composition and physical properties, such as high viscosity, corrosiveness, thermal instability, etc. Here we report a new route for producing hydrogen-rich gases together with carbonaceous materials, including carbon nanotubes, through the microwave-initiated catalytic deep dehydrogenation of coal tar using inexpensive iron catalysts. The resulting carbonaceous materials generated over the catalyst were investigated using a variety of techniques including scanning electron microscopy (SEM), transmission electron microscopy (TEM), temperature programmed oxidation (TPO) and Raman spectroscopy. Importantly, we have found that an aqueous emulsion feed of the coal tar enables considerably easier handling and an enhanced hydrogen production whilst also significantly reducing the extent of catalyst deactivation. This behaviour is shown to be assisted by the phenomenon of micro-explosion that enhances mass and heat transfer during the catalytic reactions.

Introduction

Coal tar is a major by-product arising from the coking and gasification processing of coal [1]. It is composed of a complex mixture of polycyclic aromatic hydrocarbons (PAHs), phenols and heterocyclic compounds. Although coal tar is cheap and abundant through the development of the coal chemical industry, its inherent physicochemical properties such as high viscosity, corrosiveness and thermal instability have seriously limited its application as a fuel for combustion [2]. Coal tar upgrading through hydrogenation has received a lot of interest in recent

years, with the aim of producing transportation fuels such as gasoline and diesel [3-5]. However, one of the main obstacles to restrict its widespread industrial application is the severity of the necessary reaction conditions (pressure, temperature) and high hydrogen consumption which leads to extremely high capital and CO_2 emission costs. Another drawback is the rapid catalyst deactivation arising from coke formation over any operating catalyst.

Recently, the concept of the "Decarbonization of fossil fuels" has emerged as a vital step towards to the hydrogen economy [6]. Our previous studies have demonstrated the feasibility of producing hydrogen directly from hydrocarbons such as diesel, wax and even crude oil through microwave-initiated deep dehydrogenation [7,8]. Crucially, there is no attendant CO_2 emission in such processes as they reflect a non-combustion and deep dehydrogenation of fossil fuels.

Although several attempts have been made to upgrade crude oil with microwave heating [9-11], no study to date has either investigated in detail the microwave properties and treatment of coal tar. To acquire a better knowledge of the ability of coal tar to absorb microwave energy and convert it to heat, we have measured the dielectric properties of coal tar by a microwave cavity perturbation technique. The results presented in detail in **Table A1** clearly show that coal tar is a much better microwave receptor than crude oil, most likely due to the relatively high concentration of a broad variety of polar organic molecules.

Here we therefore take advantage of this enhanced microwave absorption and report a new route to the utilization of coal tar by direct conversion via microwave-initiated catalysis into hydrogen-rich gases together with solid carbonaceous materials. Hydrogen is an attractive energy alternative to carbon-based fuels and can be utilized in high-efficiency power generation systems including fuel cells [12]. The abundant polyaromatic structures with a narrow size distribution in coal tar also make it possible to directly synthesize carbon materials like porous graphene from coal tar [13-15]. In the present study, SEM, TEM, TPO and Raman

3

spectroscopy were employed to interrogate the range of carbon species generated in microwave-initiated catalytic processing of coal tar.

The high viscosity of coal tar is of particular concern in industrial processing. In recent years a novel process of emulsion feeding has been developed in heavy oil treatment, which not only reduces the feed viscosity but also enhances the yield of light fuel oil [16]. We applied this attractive process in this study and the effects of emulsion feed on the corresponding microwave-initiated catalytic process was also investigated.

Experimental

1. Catalyst synthesis

Iron catalyst supported on activated carbon (20wt% Fe/AC) was prepared using the incipient wetness impregnation method. $Fe(NO_3)_3 \cdot 9H_2O$ (Iron (III) nitrate nonahydrate, 99%, Sigma-Aldrich) was dissolved in deionized water, then the solution was added into a desired amount of activated carbon powder (Activated Charcoal Norit®, Sigma-Aldrich) and the mixture was stirred till uniform. The sample was then dried in an oven at 110 °C overnight, followed by calcination in an argon atmosphere at 450 °C for 4 h. The catalyst was finally reduced at 700 °C for 6h in a 10% H_2/Ar flow with a space velocity of 1.67 mL(g·s)$^{-1}$.

2. Emulsion preparation

Emulsified coal tar was prepared using a high shear homogenizer with a rotator diameter of 50 mm. A composite nonionic emulsifier with a hydrophile-lipophile balance (HLB) of 4 was first dispersed in coal tar, and then a desire volume of water was added, followed by homogenization at a rotation speed of 10,000 r/m for 10 min. The volume fraction of emulsifier was 5 vol%. The coal tar was purchased from Alfa Aesar, and the crude oil samples in this study were provided by Saudi Aramco. The elemental composition of the coal tar and crude oil was given in **Table A2**. A GXML3030 Trinocular Reflected and Transmitted Light Microscope (GT Vision) was employed to observe the water-in-coal tar emulsions in this work.

3. Microwave-initiated catalytic tests

The microwave-initiated reaction apparatus was constructed in the Inorganic Chemistry Laboratory at University of Oxford (**Fig. 1**). It consists of a microwave generation and control system, a purpose-built microwave cavity and associated on-line gas chromatography [7,8]. The operating frequency is 2450 MHz (± 25 MHz) with 10% to 100% of nominal incoming microwave power. The maximum output power was 2000 W with 1% stability after thirty minutes on. The power rise time is about 100 µs.
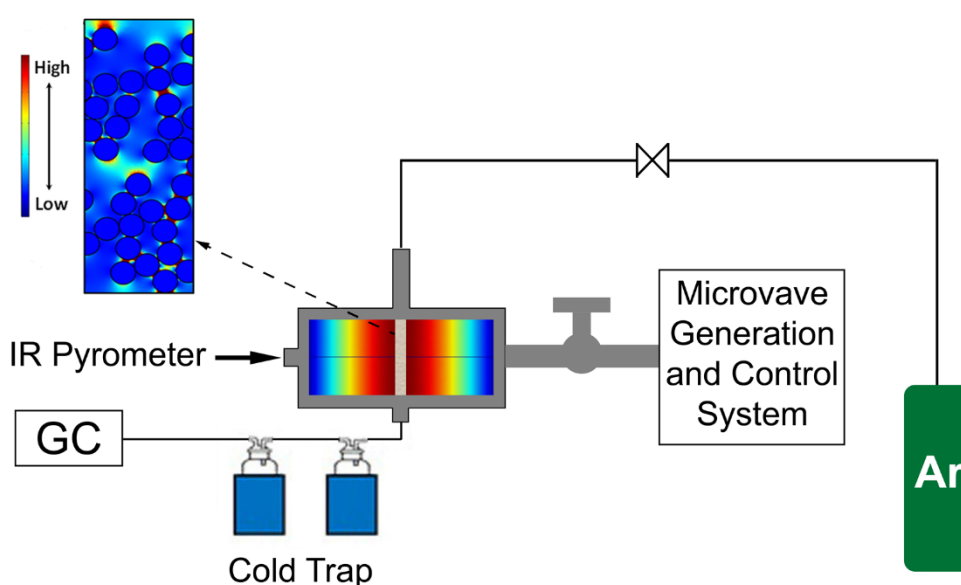
Fig. 1 Microwave-initiated reaction apparatus (not to scale, reproduced from[7,8,17]). The non-uniform energy density of electric field in the region of catalyst bed (high energy density in red, low energy density in blue) serves also to enhance the surface polarization of the individual and connected metal catalyst particles.

Initially the coal tar was melted on a hot plate and mixed with 60 wt% of freshly reduced Fe/AC catalyst. Samples with a typical volume of 3.5 cm^3 were loaded into the middle zone of the quartz tube reactor (22 cm in length and 1cm in diameter), then the system was purged with an argon flow at a rate of 1.67 mL·s^{-1} for 15 min. For each test, the sample was exposed to the microwave irradiation for 30 min. The surface temperature of the catalyst bed was measured

by an infrared (IR) pyrometer. The gaseous products were analyzed by gas chromatography using a Perkin-Elmer, Clarus 580GC fitted with TCD and FID detector. The HayeSep Q, HayeSep S, molecular sieve, silica gel and 30m*0.53 mm Col CRT- Alumina columns were used. The selectivity and yield of hydrogen were calculated using the following equations:

$$\text{Selectivity} = \frac{volume\ of\ hydrogen\ in\ gas\ products}{volume\ of\ gas\ products} \times 100\%$$

$$\text{Yield} = \frac{mass\ of\ hydrogen\ gas\ in\ gas\ products}{mass\ of\ hydrogen\ in\ reaction\ feed} \times 100\%$$

4. Characterization

^{1}H High Resolution NMR spectra were obtained on a Brüker AVIII400 (400 MHz) spectrometer using the residual solvent as an internal standard. ^{13}C NMR spectra were obtained on a Brüker AVIII400 (101 MHz) spectrometer using the residual solvent as an internal standard. Acquisitions were carried out at room temperature. $CDCl_3$ was used as the residual solvent in this work.

The morphology of the catalysts was analyzed using scanning electron microscopy (SEM) and transmission electron microscopy (TEM). SEM analysis was performed in a ZEISS EVO scanning electron microscope operated at 6 kV. TEM analysis was carried out in a JEOL JEM-2100 microscope operated at 200 kV,

Temperature programmed oxidation (TPO) was conducted in a SDT Q600 (TA instruments) thermogravimetric analyzer. TGA-DSC profiles were recorded from room temperature to 1000 °C, using a 100 mL·min^{-1} dry and oxygen-free nitrogen flow (99.99%) and 10°C·min^{-1} heating rate. For each analysis between 10 and 20 mg of sample was loaded into a small alumina crucible, using alumina as reference.

Raman spectra were collected on a Perkin-Elmer Raman Station 400F Raman Spectrometer with a scanning time of 20s. Several points of each catalyst surface were probed to explore homogeneity of the sample and reproducibility of the data.

Results and discussion

1. Gas products in the evolved gas stream

We observed that coal tar loaded on the Fe/AC catalyst from the onset of microwave irradiation rapidly released a large amount of hydrogen-rich gases. In order to investigate the effects of input power on this microwave-initiated dehydrogenation of tar oil, a series of reactions at different input microwave power from 500W to 1200W were carried out. As shown in **Fig. 2a**, the measured reaction temperature rapidly rose to 200-400 °C at the onset of microwave treatment, then it kept relatively constant during the course of the reaction. It can also be seen that the reaction temperature increased with the input (or incident) microwave power for a given (constant) irradiation time. The dominant product in the evolved gas stream was hydrogen (60-80 vol.%), together with carbon monoxide (10-30 vol.%) as well as methane (4-10 vol.%) (**Fig. 2b**). Importantly, there is very little CO_2 emitted in this process, as any residual CO_2 formed is believed to be consumed through the Reverse Water-Gas Shift (RWGS) reaction. We note that the selectivity of hydrogen has an increasing trend with the input microwave power, increasing from 65.14 vol.% at 500W to 76.83 vol.% at 1200W at an irradiation time of 30 min. This result was consistent with our previous thermodynamic studies which suggested that the deep dehydrogenation reaction is favoured at higher reaction temperature [8]. The hydrogen yields also presented an upward trend with the input microwave power (**Fig. 2c**). Therefore, we conclude that the hydrogen production is also more favourable at higher input power.
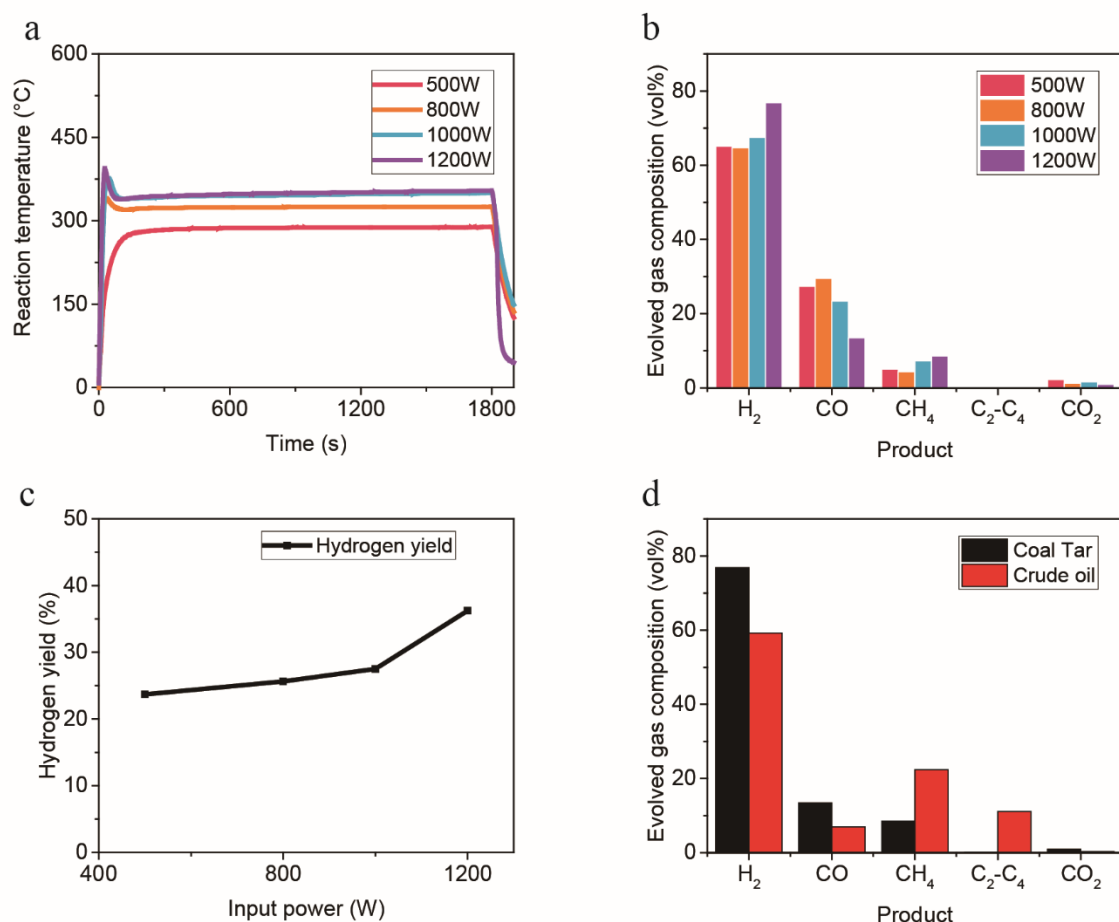
Fig. 2 a) The variation of the reaction temperature profiles with time for various incident microwave power levels. b) The evolved gas composition for coal tar dehydrogenation at input microwave power levels between 500W and 1,200W. c) The hydrogen yield for different input microwave power levels. d) The evolved gas composition for coal tar and crude oil dehydrogenation at an input microwave power of 1,200W.

Interestingly, a somewhat different product distribution was obtained when we used crude oil in the emulsion feed for microwave-initiated catalytic process. As shown in **Fig. 2d**, low chain olefins (C_2-C_4) with a selectivity of 11.13 vol.% were co-produced in the dehydrogenation of crude oil. In contrast, only a trace amount (~0.1 vol.%) of olefins were detected in the gas products for coal tar feed. Structural information as to the composition of the coal tar and crude oil was then determined by NMR spectra analysis. **Table 1** gives the assignments of the various constituent protons in ^{1}H NMR spectra [17]. As presented in **Fig. 3a**,

there exists a much higher content of aromatic protons in coal tar compared to crude oil. ^{13}C NMR spectra also demonstrated that coal tar had a considerably higher proportion of aromatic carbons; thus it can be inferred that coal tar is significantly richer in aromatic-based hydrogens. The reaction pathways for catalytic dehydrogenation of coal tar are most likely to be a competing process of the cleavage of C-H versus C-C bonds. Microwave initiation of the metal catalyst particles can lead to localised superheating at the surface of the catalyst, which may promote the scission of C-H bond on the active sites. Hence significantly higher hydrogen selectivity was obtained compared to conventional thermal cracking. The fluctuating non-uniform induced electric field in the loaded metal catalyst particles will also significantly enhance the surface polarization and consequently contribute to the hydrogen production [7].

Table 1. Assignments of proton type in ^{1}H NMR spectra

| Proton type (ppm)	Assignments
HAr (6.4-8.3)	Aromatic protons
H^{1}b and H^{2}b (0.5-2.1)	Protons of CH, CH$_2$ or CH$_3$ in the β position to the aromatic ring or further away from the aromatic ring
H^{3}b (2.1-4.3)	Protons of CH, CH$_2$ or CH$_3$ in the α position to the aromatic ring
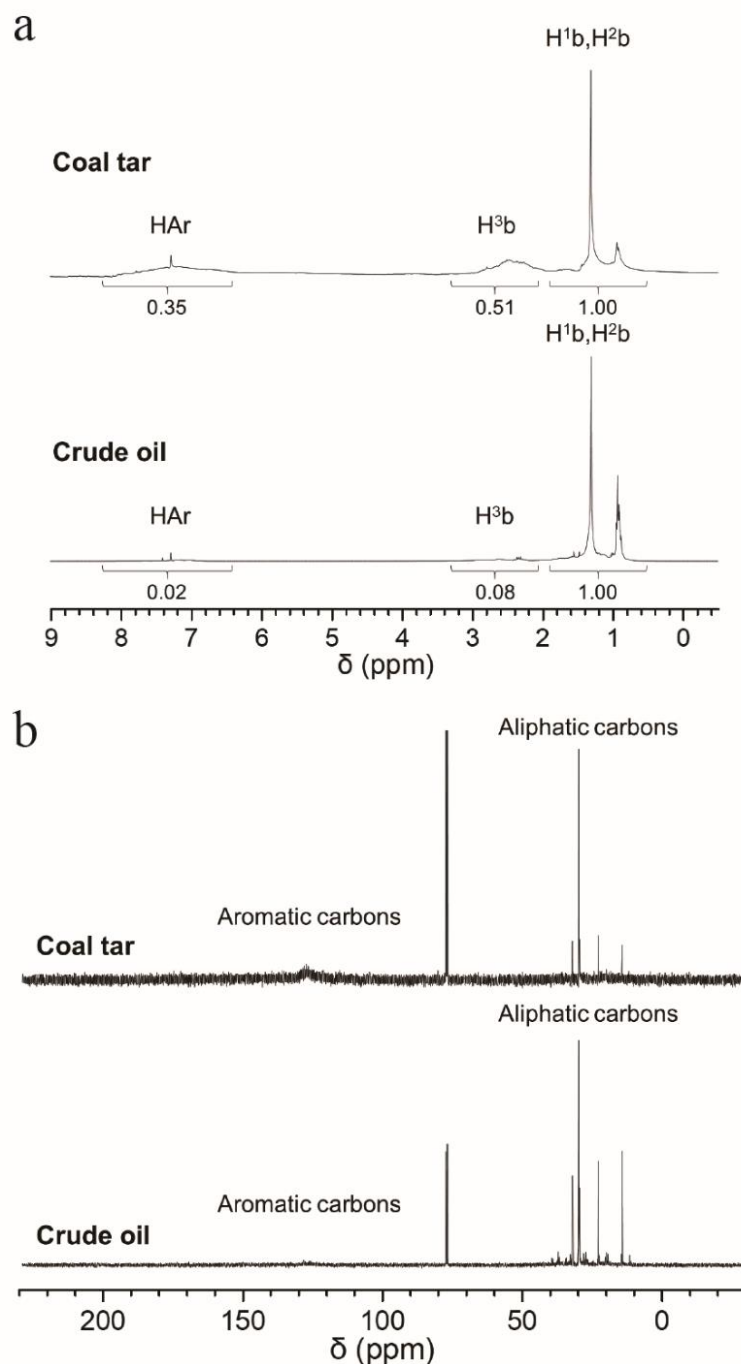
Fig. 3 a) High resolution ^1H NMR spectra of coal tar and crude oil. b) ^{13}C NMR spectra of coal tar and crude oil.

2. Carbonaceous materials generated in microwave-initiated dehydrogenation

In **Fig. 4** we show representative SEM images of the fresh Fe/AC catalyst and spent catalyst after microwave treatment at 1200W. The bright spots on the surface of the fresh catalyst

demonstrate a uniform dispersion of iron particles. These catalysts were also previously analysed by Powder XRD Diffraction and Energy Dispersive X-Ray Spectroscopy (EDS) mapping, which confirmed the presence of fully reduced and well-dispersed Fe particles on activated carbon[18]. Carbon nanotubes with curved and nano-sized filaments were observed on the surface of used catalyst （**Fig. 4c-d**） as a consequence of the carbonaceous materials produced during the microwave-initiated hydrogen generation reactions.
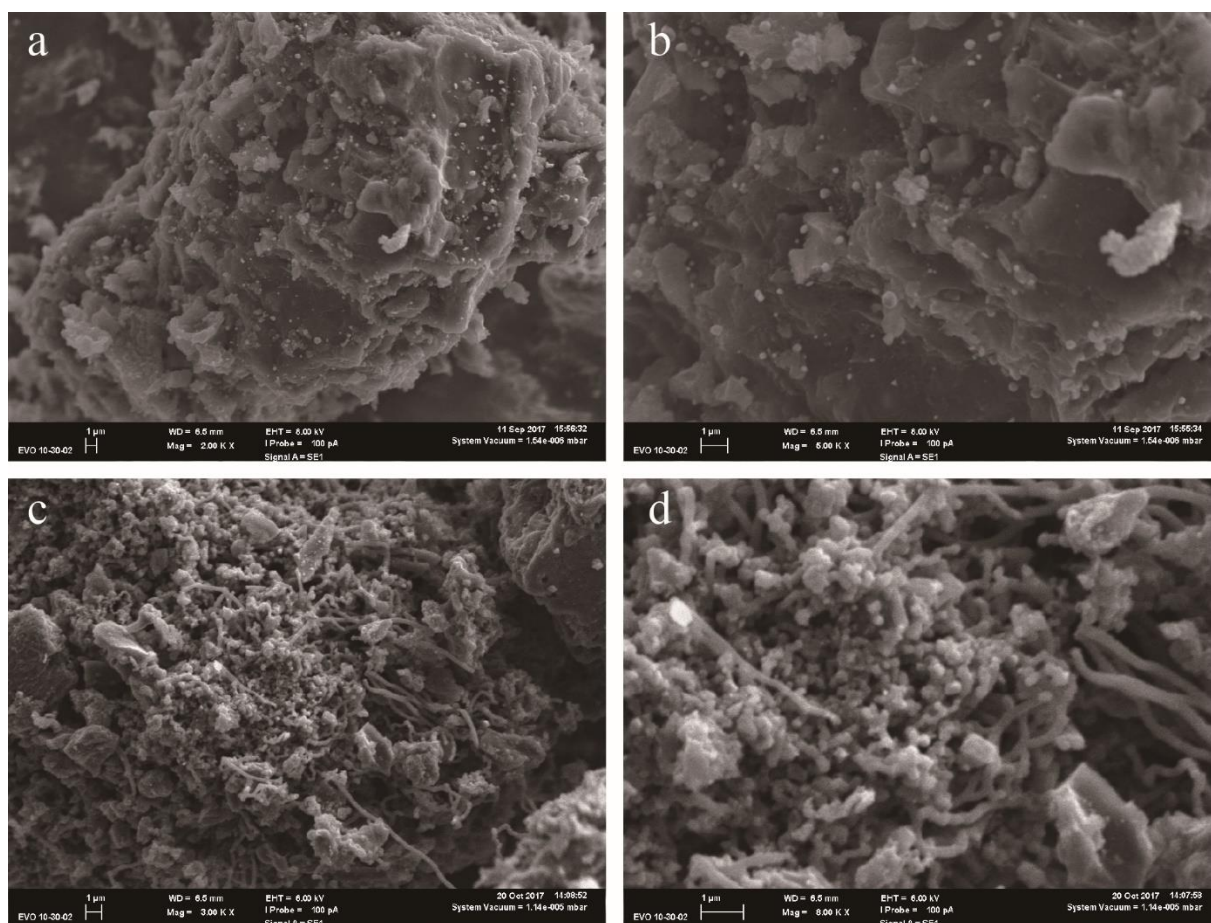
Fig. 4 Representative SEM images of the fresh and spent catalysts. a-b) Fresh 20wt% Fe/AC catalyst. c-d) Spent catalyst after microwave treatment at an input power of 1200W.

The morphological characteristics of the fresh and spent catalysts were further studied using high-resolution transmission electron microscopy (HRTEM). As shown in **Fig. 5a-b**, iron particles with a diameter of 30-100 nm were well distributed over the surface of the activated carbon support. The formation of carbon fibres over iron particles was also observed over the

11

spent catalyst. Two types of carbonaceous structures were found in HRTEM images of the spent catalysts. One is graphitic ribbons, typically with a diameter of 100nm and a length of several micrometres (**Fig. 5c**). The other is hollow nanotubes with a similar size (**Fig. 5d**). The carbon nanotubes exhibit some degree of curvature probably due to the unequal diffusion of graphitic carbon[19].
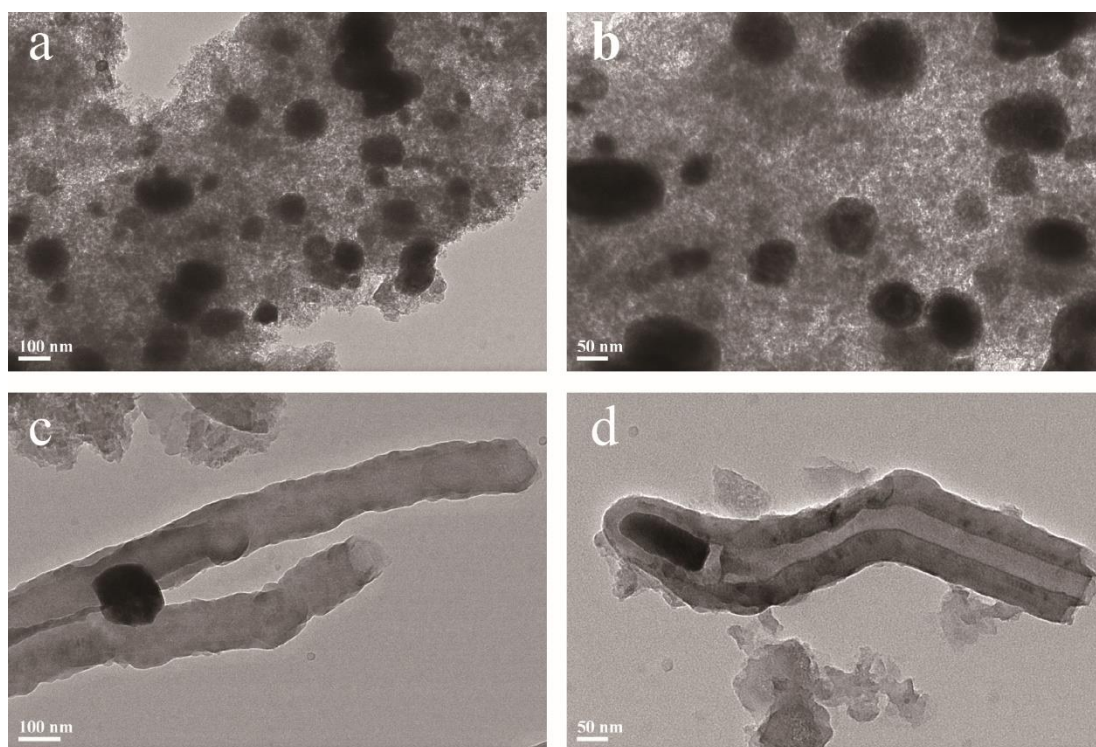

Fig. 5 a-b) HRTEM images of the fresh 20wt% Fe/AC catalyst (Taken from[17]). c-d) HRTEM images of the spent catalyst treated at an input power of 1200W.

Detailed characterizations of the carbon species generated in microwave-initiated catalytic process were performed using temperature-programmed oxidation (TPO) and Raman spectroscopy. The TPO curves of the spent catalysts have multiple peaks indicating carbon domains with different structures [20]. As illustrated in **Fig. 6a**, the oxidation temperatures of the spent catalysts are lower than that of activated carbon (~620 °C), suggesting that the produced carbon species has a less ordered structure (or a structure with large number of defects)

compared to activated carbon. We also note that the oxidation temperature of spent catalysts has a slight increasing trend with the input or incident microwave power, which indicates that carbonaceous material with a less disordered structure was generated at higher reaction temperature (i.e. input power).

The Raman spectra of the fresh and spent catalysts are given in **Fig. 7b**. The Raman band at about 1590 cm^{-1} is associated with the G peak of graphitic carbon (E2g symmetry) and the band at about 1300 cm^{-1} is attributed to A1g disorder mode (D peak) of small crystallite size of graphite-type structures[21]. A deconvolution analysis was carried out by a curve fitting procedure with appropriate band (G, D1, D2, D3, D4) combinations. In that regard we can use R1 and R2 ratios to estimate the degree of organization in carbon materials [22,23]. As presented in **Table. 2**, both the R1 and R2 ratio of spent catalysts are higher than those of fresh Fe/AC catalyst, suggesting a less organized carbon materials generated following the microwave treatment. This result is in agreement with the TPO results. A further study is therefore suggested focusing on the separation and utilization of the carbonaceous materials, for example, in manufacturing electrically conductive materials. The spent Fe/AC catalyst can also be treated through gasification with steam to produce H_2 and CO, then the hydrogen from syngas can be stored into the hydrogen pool produced from the coal tar dehydrogenation process to enrich the hydrogen production. Or the syngas can be used directly as a Fischer–Tropsch feedstock to produce high-value hydrocarbons.
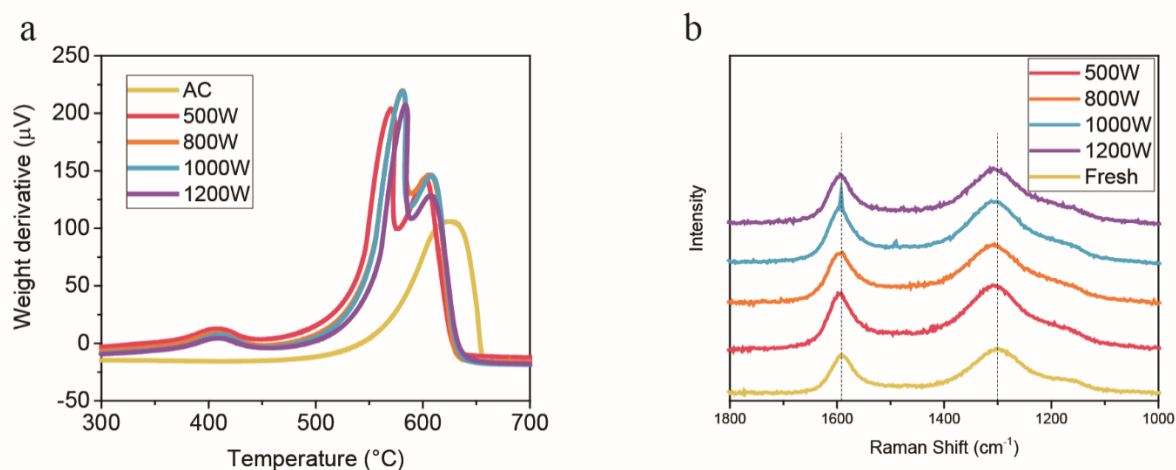
Fig. 6 a) TPO curves of the spent catalysts treated at input microwave power between 500W-1200W. b) Raman spectra of the fresh 20wt% Fe/AC catalyst and spent catalysts.

Table 2 Raman spectral parameters of fresh and spent catalysts obtained by curve fitting.

	Fresh catalyst	Spent catalyst			
		500W	800W	1000W	1200W
R1 (D1/G)	2.02	3.46	3.34	3.46	3.38
R2 (D1/(G+D1+D2)	0.67	0.68	0.68	0.69	0.67

## 3. Enhanced hydrogen production through the emulsion feed process

Since coal tar is an extremely viscous liquid which causes difficulties in storage, transportation and processing, we explored the effects of emulsification not only to reduce the feed viscosity but also to hopefully promote the degree of conversion of coal tar in the microwave-initiated catalytic process.

Stable water-in-coal tar emulsions, with low viscosity and improved flowability, were prepared using a high-speed homogenizer. A representative microscopy image of coal tar emulsions is presented in **Fig. A1**. A series of tests for emulsion feed were performed with a water content from 5 vol.% to 20 vol.%. Compared to a neat coal tar feed, emulsion feeding

led to a slightly lower hydrogen concentration and a higher CO concentration in the resulting gas products, as shown in **Fig. 7a**. However, the hydrogen yields present a slight increasing trend from 36.2% at neat tar feed to 44.8% at (15 vol.%)emulsion feed. We note that the hydrogen yield does not increase further with even higher water content in the emulsion feed, because the yields are calculated based on the total hydrogen mass in the reaction feed (including water), but only a portion of the water participated in the reactions while the rest probably escaped the catalyst bed and was collected in the cold traps.

Recharging tests were also performed to investigate the effect of emulsion feed on the catalyst deactivation, wherein the used catalysts were washed by toluene and re-loaded after each cycle. The comparison of the reaction results for solely coal tar feed and emulsified tar feed is given in **Fig. 8 a-c**. Importantly, the iron catalyst still remained active after four recharging cycles for the emulsion feed, and the decline of activity was much slower than that for neat coal tar feed. We thus conclude that the emulsion feed not only promotes the hydrogen production levels but also serves to suppress the carbonaceous deposition on the iron catalyst particles.
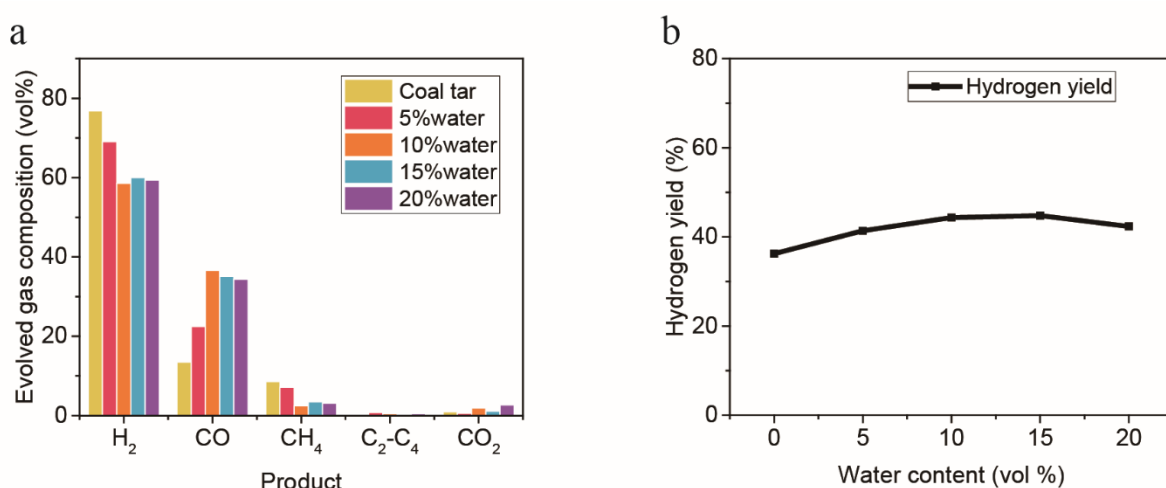
Fig. 7 The evolved gas composition and hydrogen yield of emulsified coal tar dehydrogenation with different water contents. The input microwave power is 1200W.
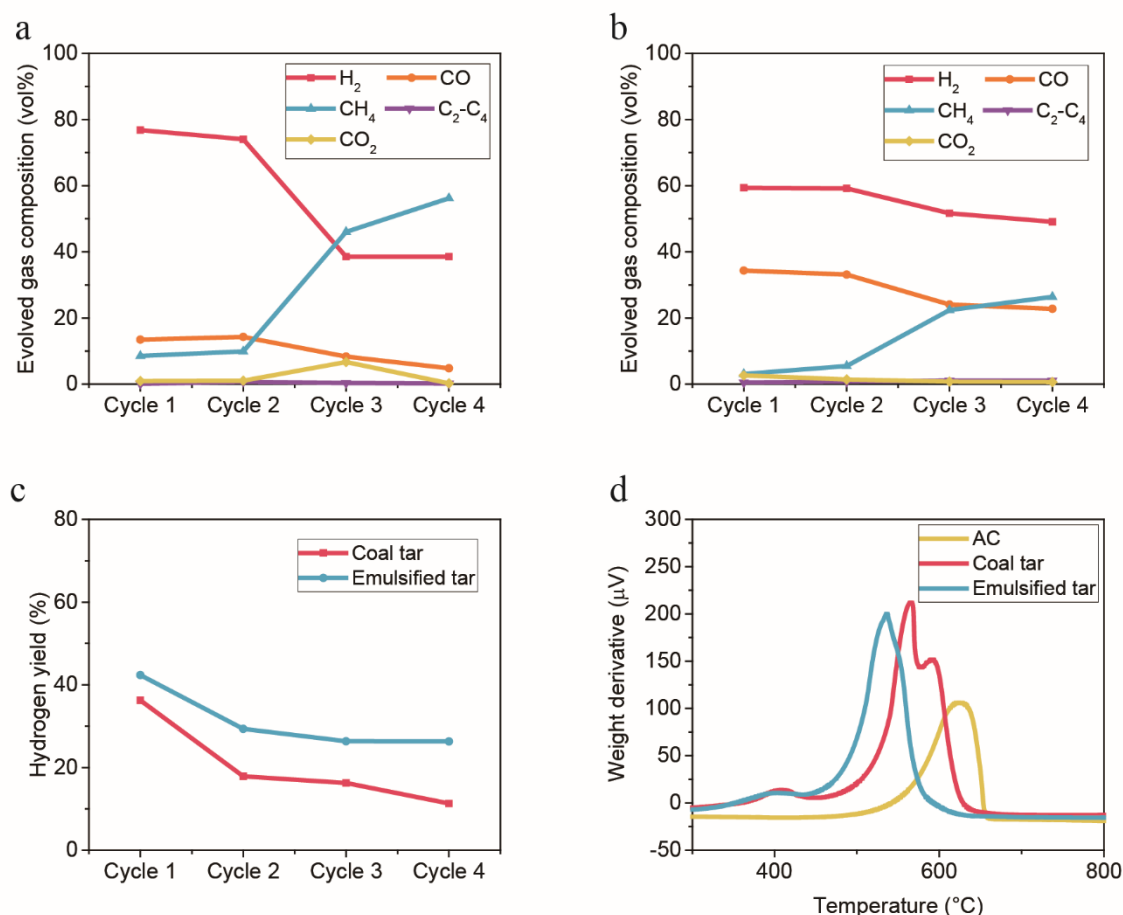
Fig. 8 Recharging catalytic reaction cycles of 20wt% Fe/AC catalyst. a) Evolved gas composition for coal tar feed. b) Evolved gas composition for emulsified tar feed. c) Comparison of the hydrogen yield for coal tar feed and emulsion feed. d) TPO curves of the fresh and spent catalysts. The input microwave power is 1200W.

Unlike conventional heating, microwaves selectively heat the microwave-absorbing activated carbon catalyst to temperatures much higher than the surroundings, which leads to the formation of hot spots at the surface of the catalyst [24]. We believe that the water vapour in the emulsion feed reacts with the carbon deposited over the catalyst particles at such a high temperature during the microwave-initiated catalytic process thereby inhibits catalyst deactivation and facilitates additional hydrogen production through the reaction: $C+H_2O \rightarrow CO+H_2$. This finding can also rationalise the significant increase of CO concentrations in gas products found for the (~35 vol.%) emulsion feed as compared to the neat

16

tar feed (~13 vol.%).

The TPO results of the spent catalysts showed carbonaceous materials with lower characteristic oxidation temperatures were generated for emulsion feeding compared to activated carbon and coal tar-derived products (**Fig. 8d**), almost certainly arising from the possible formation of large concentrations of structural defects in the carbonaceous materials.

Another factor that could also contribute to the promotion of hydrogen production is the so-called micro-explosion phenomenon[25-27]. From the onset of microwave irradiation, the water phase inside the emulsion must surely be heated rapidly due to the high dielectric loss of water at these frequencies. The water sub-droplets then begin boiling vigorously when the temperature reaches the superheating limit, followed by the massive vapour bubbling in the emulsion droplets. Subsequently the emulsion droplets are fragmentated into many tiny droplets (as illustrated schematically in **Fig. 9**). The micro-explosion can accelerate the gasification process of coal tar droplets and thus enhance mass and heat transfer during the catalytic reactions, which results in a higher conversion of coal tar feed. It was also shown that the phenomenon of micro-explosion can suppress the coke formation in catalytic cracking process [16].

Heating   **Boiling**   **Micro-explosion**
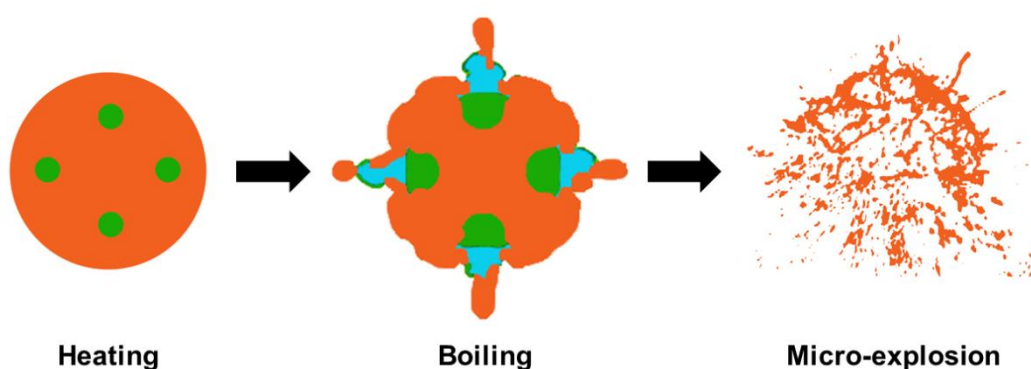
Fig. 9 Schematic for the process of micro-explosion phenomenon. The orange colour phase corresponds to coal tar, the green colour phase indicates dispersed water droplets, and the blue colour phase represents water vapor.

Conclusion

A new route to convert coal tar into hydrogen-rich gases and carbonaceous materials through microwave-initiated deep dehydrogenation was explored in this study. The dominant gas product was hydrogen, and the hydrogen production was more favourable at higher input microwave power. Carbon nanotubes, consisting of graphitic ribbons and hollow nanotubes, were generated over the iron catalyst under microwave treatment, with a less ordered structure compared to activated carbon. We also find that the emulsion feed can enhance the hydrogen production in the microwave-initiated dehydrogenation of coal tar. It also appears that the water vapor in the emulsion feed reacts with the deposited carbon on the catalyst surface thus effectively extending the period of activity of the iron catalyst. We believe that the micro-explosion phenomenon may also contribute to the promotion of hydrogen production and further studies are proceeding to investigate this aspect in detail.

References

[1] Sun M, Ma X-x, Lv B, Dai X-m, Yao Y, Liu Y-y, et al. Gradient separation of >= 300 degrees C distillate from low-temperature coal tar based on formaldehyde reactions. Fuel 2015;160:16-23.

[2] Kan T, Sun X, Wang H, Li C, Muhammad U. Production of Gasoline and Diesel from Coal Tar via Its Catalytic Hydrogenation in Serial Fixed Beds. Energy Fuels 2012;26(6):3604-11.

[3] Du J, Deng W, Li J, Li C, Du F, Zhang Z, et al. Structural and compositional evolution of coal tar toluene insoluble during slurry-phase hydrocracking. Fuel 2017;203:352-9.

[4] Li D, Li Z, Li W, Liu Q, Feng Z, Fan Z. Hydrotreating of low temperature coal tar to produce clean liquid fuels. J Anal Appl Pyrolysis 2013;100:245-52.

[5] Kan T, Wang H, He H, Li C, Zhang S. Experimental study on two-stage catalytic hydroprocessing of middle-temperature coal tar to clean liquid fuels. Fuel 2011;90(11):3404-9.

[6] Thomas JM. The enduring relevance and academic fascination of catalysis. Nature Catalysis 2018;1(1):2-5.

[7] Jie X, Gonzalez-Cortes S, Xiao T, Wang J, Yao B, Slocombe DR, et al. Rapid Production of High-Purity Hydrogen Fuel through Microwave-Promoted Deep Catalytic Dehydrogenation of Liquid Alkanes with Abundant Metals. Angrew Chem, Int Ed 2017;56(34):10170-3.

[8] Gonzalez-Cortes S, Slocombe DR, Xiao T, Aldawsari A, Yao B, Kuznetsov VL, et al. Wax: A benign hydrogen-storage material that rapidly releases H-2-rich gases through microwave-assisted catalytic decomposition. Sci Rep 2016;6:35315.

[9] Chandrasekaran S, Ramanathan S, Basak T. Microwave material processing—a review. AIChE J 2012;58(2):330-63.

[10] Li KW, Hou BC, Wang L, Cui Y. Application of Carbon Nanocatalysts in Upgrading Heavy Crude Oil Assisted with Microwave Heating. Nano Lett 2014;14(6):3002-8.

[11] Shang H, Yue YD, Zhang J, Wang JW, Shi Q, Zhang WH, et al. Effect of microwave irradiation on the viscosity of crude oil: A view at the molecular level. Fuel Process Technol 2018;170:44-52.

[12] Edwards PP, Kuznetsov VL, David WIF, Brandon NP. Hydrogen and fuel cells: Towards a sustainable energy future. Energy Policy 2008;36(12):4356-62.

[13] He X, Zhang H, Zhang H, Li X, Xiao N, Qiu J. Direct synthesis of 3D hollow porous graphene balls from coal tar pitch for high performance supercapacitors. J Mater Chem A 2014;2(46):19633-40.

[14] Wang Q, Yan J, Wei T, Feng J, Ren Y, Fan Z, et al. Two-dimensional mesoporous carbon sheet-like framework material for high-rate supercapacitors. Carbon 2013;60:481-7.

[15] Fujimoto H, Tokumitsu K, Mabuchi A, Chinnasamy N, Kasuh T. The anode performance of the hard carbon for the lithium ion battery derived from the oxygen-containing aromatic precursors. J Power Sources 2010;195(21):7452-6.

[16] Yan Y, Chen L, Xu J, Ren M, Da J, Cao F. The micro-explosion strength of emulsified heavy oil droplets in catalytic cracking process. Chem Eng Process 2016;109:90-6.

[17] Yan Y, Gonzalez-Cortes S, AlMegren H, Edwards PP, Cao F, Xiao T. Hydrogen production from crude oil with fine iron particles through microwave-initiated catalytic dehydrogenation promoted by emulsified feed. Int J Hydrogen Energy 2018;43(52):23201-8.

[18] Wang P, Jin L, Liu J, Zhu S, Hu H. Analysis of coal tar derived from pyrolysis at different atmospheres. Fuel 2013;104:14-21.

[19] Serrano-Lotina A, Daza L. Highly stable and active catalyst for hydrogen production from biogas. J Power Sources 2013;238:81-6.

[20] Alonso-Morales N, Gilarranz MA, Heras F, Rodriguez JJ, Eser S. Effects of heat treatment on the structure of LDPE-derived solid carbons. Chem Eng J 2011;172(2):1126-36.

[21] González-Cortés SL, Xiao TC, Costa PMFJ, Fontal B, Green MLH. Urea-organic matrix method: An alternative approach to prepare Co-MoS 2/γ-Al2O3 HDS catalyst. Applied Catalysis A General 2004;270(1):209-22.

[22] Sadezky A, Muckenhuber H, Grothe H, Niessner R, Pöschl U. Raman microspectroscopy of soot and related carbonaceous materials: Spectral analysis and structural information. Carbon 2005;43(8):1731-42.

[23] Beyssac O, Goffé B, Petitet J-P, Froigneux E, Moreau M, Rouzaud J-N. On the characterization of disordered and heterogeneous carbonaceous materials by Raman spectroscopy. Spectrochim Acta A 2003;59(10):2267-76.

[24] Crosswhite M, Hunt J, Southworth T, Serniak K, Ferrari A, Stiegman AE. Development of Magnetic Nanoparticles as Microwave-Specific Catalysts for the Rapid, Low-Temperature Synthesis of Formalin Solutions. ACS catal 2013;3(6):1318-23.

[25] Avulapati MM, Ganippa LC, Xia J, Megaritis A. Puffing and micro-explosion of diesel-biodiesel-ethanol blends. Fuel 2016;166:59-66.

[26] Califano V, Calabria R, Massoli P. Experimental evaluation of the effect of emulsion stability on micro-explosion phenomena for water-in-oil emulsions. Fuel 2014;117:87-94.

[27] Shinjo J, Xia J, Ganippa LC, Megaritis A. Physics of puffing and microexplosion of emulsion fuel droplets. Phys Fluids 2014;26(10):103302.

Appendix

Table A1. The dielectric properties of coal tar and crude oil samples

	Coal tar	Crude oil
Dielectric constant (ε')	2.83	2.05

Dielectric loss (ε'')	0.073	0.017
Loss tangent (tan δ)	0.026	0.008

Table A2. The elemental composition of the coal tar and crude oil

Element	Coal tar	Crude oil
Carbon (wt%)	90.85	85.40
Hydrogen (wt%)	5.46	12.70
Oxygen (wt%)	1.67	0.30
Nitrogen (wt%)	1.04	0.30
Sulphur (wt%)	0.98	1.30
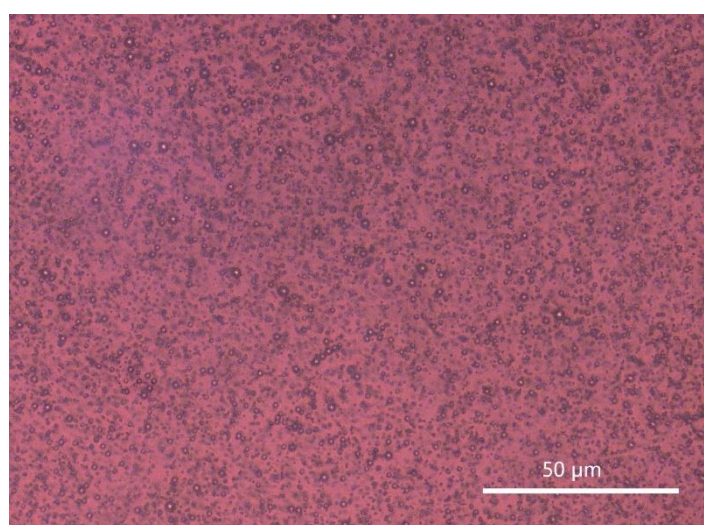
Fig. A1 Representative microscope images of water-in-coal tar emulsion.